Noncontact detection of ocular pulse—correlation with carotid stenosis

Joel L. Zuckerman, Kenneth D. Taylor, and Harry J. Grossman

Differences in ocular pulses from both eyes are well known to be associated with pathology; correlation of ocular pulse amplitude with the degree of carotid stenosis is made by a new method. Detection of ocular pulse is done by noncontact air-propagated ultrasound. Experimental results with dogs show detection of 10 to 15 percent carotid stenosis. By this method, one can screen for potential stroke in its incipient stages.

Key words: ocular pulse detection, air-propagated ultrasound, Doppler shift, phase locked loop.

With each heart beat, blood vessels supplying the eye cause a pressure wave to propagate to the cornea, producing a slight distention (1 to 50 μ) known as the ocular pulse. Alterations in ocular blood supply are reflected in parameters (i.e., shape, amplitude, duration) defining the ocular pulse.[1] Differences in ocular pulses in both eyes are associated with pathology.[2-6] By the monitoring of the ocular pulse, that class of vascular occlusive diseases causing alterations in ocular pulse become amenable to rapid early detection. We focus here on carotid stenosis.

For the last decade, there has been growing interest in the use of ultrasound for medical diagnosis. Procedures have been developed for obtaining intraocular ultrasound images as well as characteristic signals relating to intraocular structure and pathology. Circulation in the ophthalmic vascular supply has been measured by Doppler sonography. All procedures involve touching either the skin or corneal surface.[1-7] This is done primarily to minimize attenuation phenomena associated with ultrasound propagation through air. Such procedures necessarily introduce a bias pressure on the eye by virtue of mechanical contact or elevated pressure in the coupling medium. This attenuates fine structure present in the eye's unbiased motion.

Our procedure uses ambient air as the coupling medium between the acoustic transducer and the corneal surface. Use is made of the large impedance mismatch between air and corneal tissue to obtain more than 99% of the incident energy in the reflected beam. Motion of the eye, due in particular to the ocular pulse, is detected as a Doppler shift of the incident frequency. As a result, fine structure involved in the eye's dynamic motion is seen. These dynamics include motion of the eye as a function

From the Department of Surgery, Saint Francis Hospital and Medical Center, Hartford, Conn., and the National Data Systems, Hartford, Conn.

Submitted for publication April 26, 1977.

Reprint requests: Joel L. Zuckerman, M.D., Department of Ophthalmology and Visual Science, Yale University, 333 Cedar St., New Haven, Conn. 06510.

of the elastic properties of corneal tissue, mechanical motions of intraocular medium, and spatial distribution of ocular blood flow.

Materials and methods

General description. The change in reflected carrier frequency (Δf) of an incident wave front striking a moving surface (Fig. 1) is known as the Doppler shift and is given by the following equation:

$$\Delta f = 2f \frac{v}{c} \cos \theta \qquad (1)$$

where Δf = change in carrier frequency f, v = velocity of object being interrogated, c = velocity of sound in the media, and θ = angle of incidence of the wave front.

Thus, as the cornea is displaced in time by the intraocular pulse pressure, we obtain a change in frequency of the reflected wave front. Detection and demodulation of the shifted frequency yield the corneal velocity. To obtain the corneal displacement, we perform an integration.

We have developed a concentric, ultrasonic probe that uses ambient air as the coupling medium between transducer and corneal surface. Functioning in a continuous wave mode at 1 mHz, Doppler-shifted signals are obtained from the moving corneal surface. Our system can detect a corneal displacement as small as 5 μ. The probe focuses the ultrasound to a 3 mm. beam diameter at 20 mm. focal length, with 15 mm. depth of field. In use, the probe is situated 2 to 4 cm. from the patient's eye, absolute positioning being unimportant because signals are frequency, not intensity, dependent. The head is accommodated by a chin and forehead rest, and the patient stares at a small fixed light. This configuration eliminates noise secondary to eye and head motion. Alignment takes a few seconds, and measurements, 5 to 10 sec. An example of human ocular pulses is shown in Fig. 2. The ocular pulse in this subject is seen to be biphasic. Simultaneous ipsilateral carotid pulse, ECG, and 1 sec. time markers are included for reference purposes.

Description of system. We refer to the block diagram of the operating system as shown in Fig. 3. The system is described in seven discrete but interconnected operational blocks as follows.

Power oscillator. We interrogate the corneal surface via the transducer with a continuous sinusoidal voltage at the frequency f produced by a power oscillator. The voltage is of the form $A_1 \sin(\omega t)$, where ω equals $2\pi f$ and A_1 is the amplitude. This voltage drives the ultrasonic transducer *(T)*, producing the ultrasonic beam propagated to the surface of the eye.

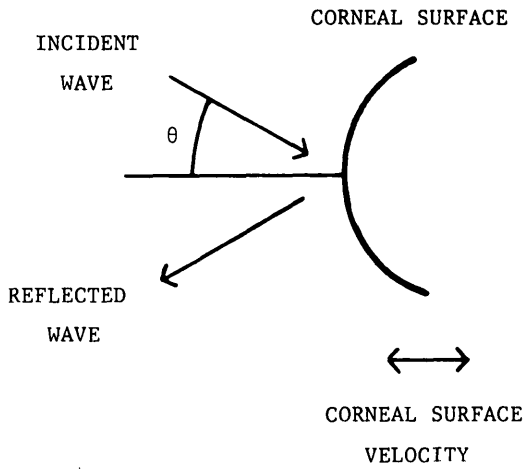

Fig. 1. Vector representation of ultrasound propagation at the corneal surface. The θ represents the angle of incidence of the ultrasonic beam.

Ultrasonic transducer. This is a two-stage device for transmitting and receiving.

The center segment is a focused transmitter which produces an ultrasonic beam between 2 to 3 mm. in diameter at a distance of 20 mm. from the transducer surface. The transmitted ultrasonic beam appears to be collimated over the distance of interest along its depth of field, which is approximately 15 mm. The beam is reflected from the moving corneal surface and received by the focused receiving segment.

The receiving segment is a focused spherical receiver whose center has been removed and in which the transmitter is concentrically positioned. Once the incident carrier wave strikes the eye surface, it becomes frequency modulated (FM) due to the Doppler frequency shift. It is the Doppler-shifted carrier that is sensed by the focused spherical receiving section. The received signal is coupled into a bandwidth limited amplifier (A-1). Our signal is now of the form $A_2 \sin[(\omega \pm \Delta\omega)t]$, where $\Delta\omega = 2\pi\Delta f$ and A_2 is the peak amplitude of the return signal.

Amplifier A-1. The input signal $\{A_2\sin[(\omega \pm \Delta\omega)t]\}$ to A-1 is multiplied by a varying gain $[G(A_1)]$ which is proportional to the amplitude of the input signal. This provides automatic gain control for the received signal. The output of A-1 is now gain controlled, bandwidth limited, and represented by $G(A_1)A_2 \sin[(\omega \pm \Delta\omega)t]$ and is sharply attenuated outside of the amplifier's passband. We are now ready to demodulate the FM signal, which is done by the phase locked loop (A-2).

Phase locked loop (A-2). A-2 is a phase locked loop (PLL) whose output is proportional to the change in the frequency of the input signal.[8]

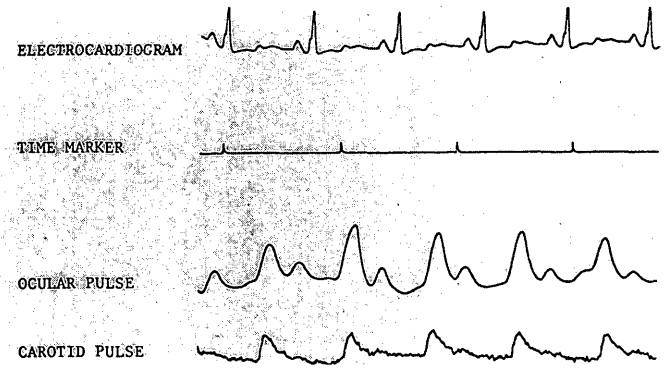

Fig. 2. Human ocular pulse experiment. Time marker indicates 1 sec.

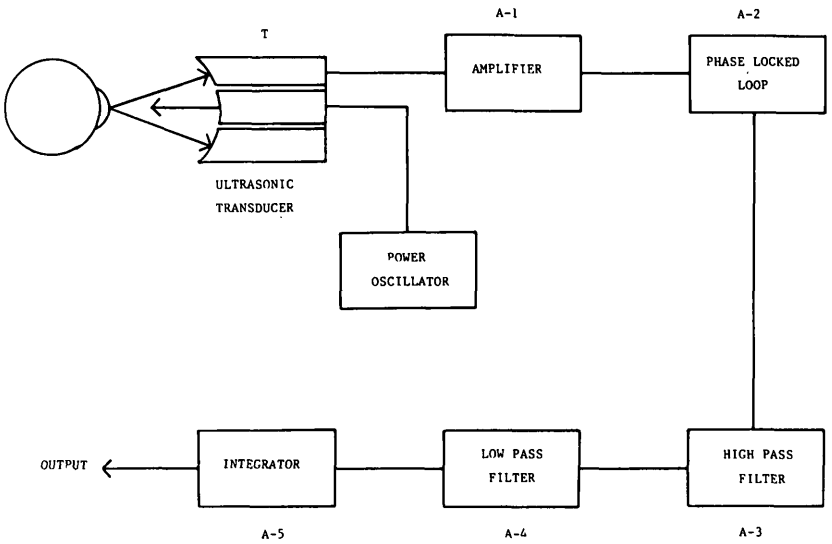

Fig. 3. Block diagram of the ocular pulse detection system.

The change in output voltage is given as follows:

$$\Delta V = \Delta\omega/K \qquad (2)$$

where ΔV is the change in the PLL demodulated output voltage, $\Delta\omega$ is the change in the input carrier frequency, and K is the conversion gain of the PLL's voltage-controlled oscillator (VCO).

By combining equations 1 and 2, the output voltage is given:

$$\Delta V = \frac{4\pi v \cos\theta}{cK} \qquad (3)$$

If we assume that θ is constant, the angular variable ($\cos\theta$) is constant. In practice, this has been realizable. The velocity (c) of the ultrasound in ambient air is constant. Thus the PLL demodulated output is proportional to the velocity of the corneal surface.

It should be noted that this voltage may contain unwanted artifact, which can be introduced in the following two ways: (1) a slow varying motion in either the ambient air or the surface being interrogated, which shows up as a very low frequency signal on which the velocity is superimposed, or (2) the high-frequency (1 mHz) low-amplitude reference signals used to do phase comparison in the PLL. This low amplitude signal rides on the PLL demodulated signal. These unwanted artifact components are reduced by amplifiers A-3 and A-4.

Amplifiers A-3 and A-4. These are unity-gain, high-pass and low-pass filters, respectively. The function of A-3 is to provide a flat-frequency pass band above a low-frequency cut-off point. This high-pass action removes the slow, varying low-frequency component of the demodulated FM signal. In contrast, A-4 provides a flat-frequency pass band below a high-frequency cut-off point. This low-pass action removes the high-frequency

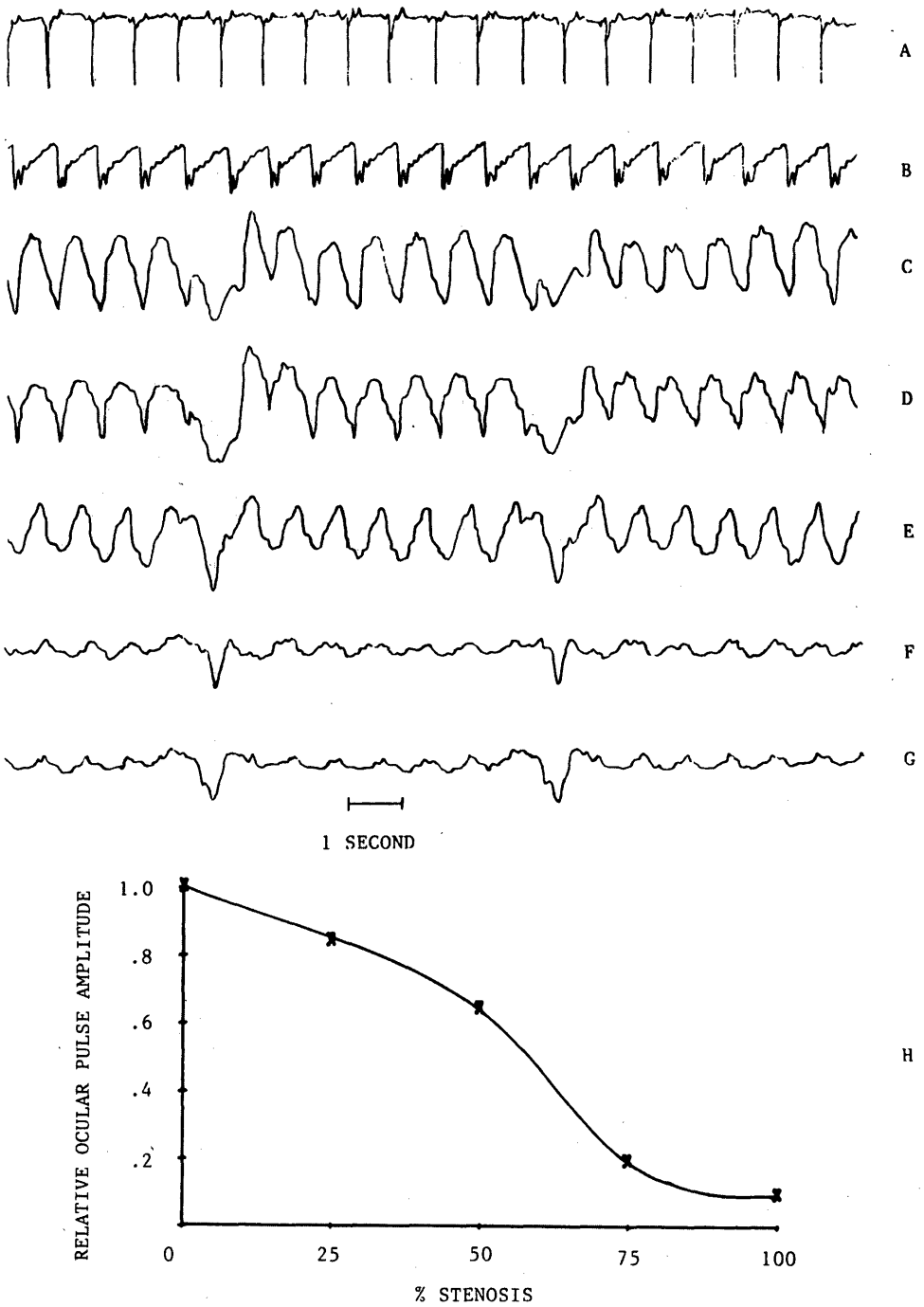

Fig. 4. Canine ocular pulse at varying degrees of stenosis. *A* and *B*, ECG and intra-aortic pressure waves, respectively. Note that these are inverted relative to the ocular pulses (curves *C* to *G*). *C*, Ocular pulse at 0 percent carotid artery stenosis, synchronized with simultaneous ECG and aortic pressure pulses. Note the two artifactual areas after the fourth and eleventh pulses. These represent respiratory efforts introduced by the Bird respirator. All subsequent ocular pulses are synchronized with the respiratory pulses. *D* to *G*, Ipsilateral carotid artery stenosis of 25, 50, 75, and 100 percent, respectively. *H*, Ocular pulse amplitude relative to that at 0 percent stenosis, versus percent stenosis. Chart speed is 10 mm./sec.

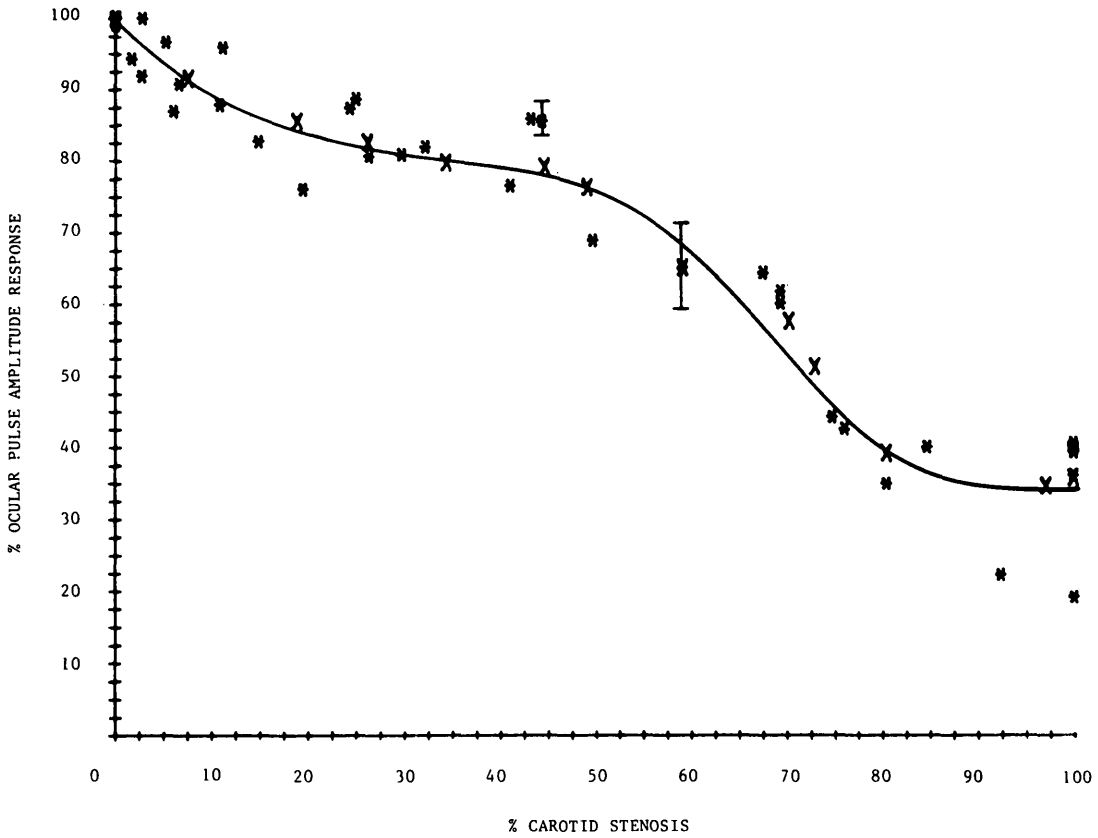

Fig. 5. Normalized ocular pulse amplitude vs. percent carotid stenosis. Asterisks represent data points for individual dogs, and X data points and solid line form the average value plot for all dogs.

reference signal from the demodulated FM output signal. With amplifiers A-3 and A-4 in cascade, the over-all transfer function is that of a band pass filter. The artifact components of the demodulated signal have been significantly reduced to yield a signal/noise ratio greater than 40 dB.

Integrator. To obtain the displacement of the cornea, we integrate the velocity signal. This is accomplished by amplifier A-5 which is an AC integrator. However, the time domain response is that of a single-pole resistance-capacitance filter rather than a true integral. This procedure provides DC amplifier stability. The output of amplifier A-5 is a voltage proportional to the corneal displacement.

Correlation with carotid stenosis. Six healthy mongrel dogs, 20 to 25 kg., were premedicated with Innovar-Vet (0.25 cc./kg.) and anesthetized with sodium pentobarbital (25 mg./kg.) and Flaxedil (0.1 mg./kg.). Each animal was intubated and placed on a positive-pressure respirator. Lead II ECG and central aortic blood pressure were monitored. With sterile technique, one common carotid artery was exposed just below the bifurcation and systematically ligated with a vascular clamp.

The ipsilateral eye was fully exposed by suturing back the lid, and the ultrasonic transducer was positioned 2 cm. from it. The eye was irrigated periodically with sterile saline. The vessel was gradually occluded with a Blalock clamp while the carotid arterial area, ocular pulse, aortic pressure, and ECG were simultaneously recorded.

Experimental results

The result of a typical carotid stenosis experiment is shown in Fig. 4. Data points in Fig. 4, *H*, were obtained in the following manner. Under compression, the vascular clamp caused the arterial cross-section to appear as a rectangle with two semicircles on its ends to good approximation. The ratio of carotid area at arbitrary compression, to open circular area is given as follows:

$$A/A_o = 1 - \varepsilon^2 \text{ and } \varepsilon = a/d \qquad (4)$$

where d is the inside diameter of the artery and a the linear distance travelled by the clamp. The carotid stenosis is therefore ε^2. For each arterial opening, the average of 10 to 20 ocular pulse amplitudes were calculated. These values were normalized to the average open artery ocular pulse amplitude. The percent of ocular pulse amplitude response is plotted versus the percent of carotid stenosis.

Fig. 5 collates the results of six dogs. The asterisk data points are the individual values of each dog. Accuracy in the percent of stenosis was 4.08 percent. Thus we averaged the asterisk data points over an interval of 8.16 percent, the average being weighted by the positions of data points within the interval. These are the *X* data points and solid line. Average root mean square (RMS) fluctuations in the asterisk data points were ± 2.5 percent. Average RMS fluctuations in the X points was 6 percent.

Discussion

Best and others[1-7] have shown that the ocular pulse amplitude is correlated with the degree of carotid stenosis. We substantiate these findings also, as shown in Fig. 4. Obvious decreases of amplitude occur as the carotid artery is closed. In addition, the ocular pulse generally mirrors the aortic pressure wave shape and duration. Distortions are expected as a result of dispersion introduced by the elastic and other properties of the eye through which the ocular pulse propagates. However, such distortions are not severe until the carotid artery is nearly closed. At total closure, a small ocular pulse is still present, which represents retrograde flow to the eye through the circle of Willis. This result has importance in neurological applications where it is desired to assess the patency of intracranial vessels.

Our technique demonstrates that carotid stenosis in a given individual as small as 10 to 15 percent is observable (Fig. 4, *H*). This represents a factor of four to five times more sensitivity than that reported in current literature. Ocular pulse is shown therefore to be a more sensitive indicator of carotid stenosis than previously suspected. Marked fall-off in ocular pulse amplitude beyond 50 percent carotid closure has been noted by others. Detection of ocular pulse by air-propagated ultrasound also supports this data (Figs. 4 and 5).

It should be noted that Fig. 5 represents aggregate data from several dogs. These dogs had a wide distribution of ages, size, blood pressure, cardiovascular status, and general condition. Significantly, there is relatively little dispersion in the data. Larger sample size and control of these parameters should therefore define calibration curves against which an individual can be measured. The time evolution of a given individual's status can now be determined by sequential measurements.

Summary

Noncontact ocular pulse detection by Doppler-shifted air-propagated ultrasound has been described. Correlation of ocular pulse amplitude with carotid stenosis has been made in a small population of dogs. For a given individual, stenosis of 10 to 15 percent is detectable. Extension of our procedure to binocular recording and adaptation for human use, especially in those scheduled for carotid angiography, is currently in progress.

We thank Mr. John Piquette and Mr. Gilberto Vega of the Cardiovascular Research Laboratory, St. Francis Hospital and Medical Center, Hartford, Conn., for their assistance with the canine experiments and Mrs. Claire Martin for typing the manuscript.

REFERENCES

1. Best, M., Pola, R., Plechaty, G., Masket, S., and Galin, M. A.: Ocular pulse studies in carotid stenosis, Arch. Ophthalmol. **85**:730, 1971.
2. Best, M., Keyes, M., Plechaty, G., and Galin, M. A.: Graphic analysis of the ocular pulse in carotid occlusion, Arch. Ophthalmol. **85**: 315, 1971.
3. Best, M., Plechaty, G., Harris, L., and Galin, M. A.: Ophthalmodynamometry and ocular pulse studies in carotid occlusion, Arch. Ophthalmol. **85**:334, 1971.

4. Bynke, H. G.: Screening diagnosis of carotid occlusion by means of oculosphygmography, Neurology **16**:383, 1966.
5. Sand, B. J., Barker, W. F., Freeman, L. W., and Hummell, S.: Ophthalmic arterial blood pressures measured by ocular pneumoplethysmography, Arch. Surg. **110**:813, 1975.
6. Gee, W., Mohigan, J. T., and Wylie, E. J.: Measurement of collateral hemispheric blood pressure by ocular pneumoplethysmography, Am. J. Surg. **130**:121, 1975.
7. Bron, A. J., Knox, D. L., and Gaasterland, D.: Tomographic studies in carotid occlusive disease, Br. J. Ophthalmol. **1**:577, 1971.
8. Gardner, F.: Phaselock techniques, New York, 1966, John Wiley & Sons, Inc.

Notice to Contributors

After October 1, 1977, please submit all manuscripts to:

Alan M. Laties, M.D., Editor
Investigative Ophthalmology & Visual Science
Room 620
Scheie Institute
Myrin Circle, 51 N. 39th St.
Philadelphia, Pa. 19104

Dr. Laties will assume editorship of the JOURNAL as of January 1, 1978.